INSTITUTE OF PLASMA PHYSICS

NAGOYA UNIVERSITY

RESEARCH REPORT

NAGOYA, JAPAN

Experiment on STP, an Axisymmetric Fast Toroidal Pinch with Very Small Aspect Ratio†

K. Hirano, S. Kitagawa, M. Mimura, Y. Kita,
M. Ohi*, T. Amano* and M. Wakatani**

IPPJ-197 October 1974

Further communication about this report is to be sent to the Research Information Center, Institute of Plasma Physics, Nagoya University, Nagoya, Japan.

---

† Paper to be presented in the Fifth International Conference on Plasma Physics and Controlled Nuclear Fusion Research.

* Permanent address: Plasma Physics Laboratory, Faculty of Engineering, Osaka University, Osaka.

** Permanent address: Japan Atomic Energy Research Institute.

IAEA-CN-33/E9-5

Experiment on STP, an Axisymmetric Fast Toroidal Pinch with Very Small Aspect Ratio

Kei-ichi HIRANO, Shiro KITAGAWA, Mikio MIMURA,
Yoshio KITA, Masakazu OHI*, Tuneo AMANO* and
Masahiro WAKATANI**

Institute of Plasma Physics, Nagoya University,
Nagoya, Japan

---

* On leave from Plasma Physics Laboratory, Osaka University

** On leave from Japan Atomic Energy Research Institute

Abstract

A high β fat tokamak configuration operated under a small q value is tested. The maximum ion and electron temperatures are 500 and 100 ev, respectively, while a plasma density about $1 \times 10^{15}/cm^3$ is observed. A violent toroidal drift appears after the pinch implosion and a large amount of the plasma energy is lost within 10 μsec. However, application of pulsed vertical field of about 480 G dramatically changes this situation. The movable magnetic probe measurements show that, with the vertical field, the plasma pressure at 17.6 μsec after the start of the main discharge is 3×10^{17} eV/cm^3, whereas, it becomes very small when the field is not excited. Large signals of m = 2 mode appear when the B_p signal of eight pick-up loops around the minor circumference of the torus is transformed into Fourier components. The m = 2 mode becoms small when the high β operation with negative bias field is done. It is also observed the sine component of m = 1 mode appears when the q value is increased to 2 from 1.3. These phenomena can be explained qualitatively by the theory of Freidberg and Haas.

The success of θ-pinch experiments is encouraging and driving the study of toroidal pinches in order to achive higher position on $n\tau$-T diagram. Among various existing high β pinch torii, axisymmetirc configuration is one of the most fundamental ones. Depending on how to stabilize the plasma, there appeared several different proposals, such as the reverse field HβTX pinch[1], the screw pinch[2], the high β pinch tokamak[3], and the non circular belt pinch[4]. The STP, symmetric toroidal pinch, is constructed to test all of these circular configurations. In the present paper, however, the efforts are mainly concentrated on the high β tokamak configuration to challenge the density and temperature limits observed in usual tokamak discharges. Since the equilibrium theory shows that the maximum β of STP operated under tokamak mode does not exceed 20% ($1/2Aq^2$), reduction of β attained in θ-pinch experiments becomes important. A low pressure operation of a torus is effective to reduce β without also lowering the plasma temperature. In the STP discharge, the plasma experiences three different phases; phase-1 (plasma production and pinch phase), phase-2 (transient phase in which the plasma oscillates around the equilibrium axis), and phase-3 (quasi-static equilibrium phase). In most cases, the plasma goes into the phase-3 about 10 μsec after the beginning of the discharge. Since the plasma in the phase-3 has already been reported[5], attention is paid here to the phase-2. The plasma in the phase-2 is observed by various diagnostic tools and the results are compared with the theory of Freidberg and Haas[5]. In order to suppress a violent toroidal drift which appears at the end of the phase-1, pulsed vertical field whose waveform is similar to that of plasma current is applied.

A schematic drawing of the STP-system is shown in Fig.1. The major dimensions and parameters are indicated in Table I. As can be seen, double copper shell structure is adopted in order to cancel the error field generated by the tub of the induction coil, which is the primary winding for driving the plasma current. Eight vertical field coils are fitted inside the copper shell. In order not to give any induction to the plasma current, the vertical field coils are re-wound just outside the shell. Therefore, the vertical field can be generated independently of the plasma current. The operating D_2 gas, admitted through a fast acting gas valve, is usually filled up to 10^{-2} Torr. Figure 2 shows typical waveforms of the plasma current I_p and main toroidal magnetic field B_t. It has been found that the decay of the plasma current results mainly from external circuit resistance[5]. In order to generate smooth current curve as shown in Fig.2, crowbar timing of B_t circuit is important. If the timing of B_t is improper, a large dip appears at the peak of the plasma current. Plasma parameters are measured by various ways. Electron temperature is measured by laser scattering, soft X-ray foil absorption and transient characteristic of impurity lines. Temperatures of ions are estimated by neutral particle energy analyzer, Doppler broading of D_α and O-IV-3063 Å line. Typical output signals from neutral particle analyzer with and without plasma current are illustrated in Fig.3. It can be seen that the plasma confinement is evidently improved by generating the plasma current along the major circumference of the torus. The energy spectrum of the neutral partcles shows two components of different temperatures. A typical Doppler profile of D_α line is shown in Fig.4. It is not surprising that the D_α line also shows two component temperatures. Plasma density is obtained by laser scattering and a mass oscillation frequency. Under a typical operating condition, in which B_t is 7 kG and I_p is 105 kA, the time evolution of the plasma parameters are measured by various techniques mentioned above. The results are summarized in Fig.5. The agreement between different measuring techniques seems to be reasonable, except for the discrepancy seen in the electron temperature obtained by laser scattering and foil absorption soft X-rays technique. It is noted that the plasma density obtained by laser scattering and mass oscillation is in agreement approximately with the filling pressure number density of $7 \times 10^{14}/cm^3$. In the case when B_t is raised to 10.5 kG with also increasing I_p to 140 kA, the maximum ion and electron temperatures become 500 and 100 eV, respectively. It is observed, that electrons are cooled down rapidly within 10 μsec, whereas the ion temperature is still about 200 eV at 15 μsec after the start of the discharge. The β value and plasma pressure distributions are obtained by movable magnetic probes. The β value can also be obtained by a diamagnetic loop and eight magnetic probes installed around the minor circumference of the discharge tube. The discrepancy of the β value obtained by the above different methods is found to be small. The shape and macroscopic motion of the plasma is observed by the eight magnetic probes. As shown in Fig.6, the B_p signals from the probes are put into a Fourier analyzer and are transformed into five Fourier components; m = 0, sine and cosine components of m = 1 and 2. Here, in order to save the number of amplifiers required, the origin of azimuthal angle θ is turned 22.5° chockwise from the horizontal mid plane.

A typical example of the output signal from the Fourier analyzer is shown in Fig.7. As can be seen, the dominant harmonic components are a_1(m = 1 cosine component) and b_2(m = 2 sine component). The oscillation which appears on a_1 is understood by the radial oscillation around the equilibrium axis, the frequency of which is given by[7]

$$f = \frac{1}{2\pi}\sqrt{\frac{\mu_0 \ I_p^2}{2\pi M(b^2 - a^2)}} \ ,$$

where, M is the mass per unit length, a and b are the plasma and shell radii, respectively. In case a/b = 0.7, observed frequency gives the value of M the mass of the filling gas. The appearance of large m = 2 mode suggests the elliptic deformation of the plasma. The deformation can not be related to the usual equilibrium distortion of the plasma, since the observed major axis of the ellipse is slanted about 45° to the major axis of the torus. The deformation may be due to some instability. Since, the safety factor q is chosen to be 1.2 at the discharge tube wall in this operation, expected dominant harmonic of kink mode is m = 1 according to the straight cylindrical model[8][9]. However, Freidberg and Haas[6] showed theoretically that the toroidal effect is important for kink mode and the dominant harmonic of marginal state is m = 2. The observed elliptic deformation may possibly be related to their theory. In order to confirm the theory, the average β and the surface q value are changed. The results are given in Fig.8, in which the time evolution of q, β, the amplitude of m = 2 mode $\sqrt{(a_2^2 + b_2^2)/d_0^2}$ and the m = 1 sine component (b_1/d_0) are plotted for three different operating conditions. As can be seen, when the β is high, the m = 2 mode disappears before 10 μsec (operation B), while in the case of low β operation, the m = 2 mode remains to be the dominant mode (operation A). In the case q is increased to around 2, sine component of the m = 1 mode becomes significant. These tendency is qualitatively in agreement with the prediction of Freidberg and Haas, at least. The pulsed vertical field of 480 G is applied. The field is shaped to be the same waveform as that of the plasma current. A dramatic improvement of the plasma confinement is observed. The time evolution of the pressure distribution is seen in Fig.9. Since the plasma density is not more than $7 \times 10^{14}/cm^3$ or the filling pressure, the plasma temperature at 17.6 μsec after the main discharge would not be lower than 200 eV. As can be seen, the plasma is shifted to the inner wall. This will be corrected by more adequate choice of pulsed vertical field waveform. The amplitude of m = 2 mode for this operation is shown in Fig.10. As is expected, larger m = 2 mode appears in the operation without vertical field, because the β is smaller when the vertical field is not applied. The m = 2 mode peaks at 9 μsec after the start of the discharge. At this instant the plasma seems to touch the tube wall violently, because strong light emission is observed on the streak photographs. The distribution of the plasma current for this operation is shown in Fig.11. The skin current structure at 4.7 μsec after the start of the discharge is quickly destroyed and the sharply peaked structure appears at 7.1 μsec. The peaked current distribution is somewhat broadened after the m = 2 peaking. It should be noted that the small second current peak and reverse current begin to appear near the inside periphery of the torus. This small peak grows up considerably at 17.6 μsec. In the case when the vertical field is applied, sharply peaked current distribution does not appear and, consequently, no peaking of m = 2 mode. These process may have some connection to the disruptive instability which appears in ordinary tokamaks.

In the phase-2, plasma current distribution is usually of skin shape, which leads to the apparent agreement of the experimental results with the theory of Freidberg and Haas. It can be said that for stable confinement β value must not be too high nor too low. It it found that the role of the pulsed vertical field is very important. At present, however, only preliminary results are obtained. Further efforts will be paid for optimizing the vertical field effects.

The authors acknowledge the technical assistance of Mr. M. Kusagaya, Mr. S. Yamada and Mr. T. Naito. They are grateful to Mr. S. Ushio for his help in designing the neutral particle analyzer and SX foil absorption system. They would like to thank to Professor H. Yoshimura and Professor K. Takayama for their continuous encouragement.

References

[1] H. A. B. BODIN, E. P. BUTT, J. E. CROW, F. E. IRONS, J. JUNKER, A. A. NEUTON, and D. C. ROBINSON; in Proceedings of Fourth International Conference on Plasma Physics and Controlled Nuclear Fusion Research, Madison, Wisconsin, 1971 (International Atomic Energy Agency Vienna 1972), Vol.I, p. 225.

[2] P. C. T. VAN DER LAAN, W. SCHUURMAN, J. W. A. ZWART, and J. P. COEDBLOED; ibid. Vol.I, p.217.

[3] H. J. BELITZ, L. JANICKE, P. NOLL, U. PLANTIKOW, F. SAND, J. SCHLÜTER, F. WAELBROECK, and G. WAIDMANN; ibid. Vol.III, p.179.

[4] R. WILHELM and H. ZWICKER; ibid. Vol.I, p.259.

[5] K. HIRANO, S. KITAGAWA, and M. MIMURA; Phys. Rev. Letters 32 1104 (1974).

[6] J. P. FREIDBERG and HAAS; Phys. of Fluid. 16 1909 (1973).

[7] V. S. MUKHOVATOV and V. D. SHAFRANOV; Nuclear Fusion 11 605 (1971).

[8] V. D. SHAFRANOV; Zh, Tekh, Fiz. 40 241 (1970) [Sov. Phys. Tech. Phys. 15 172 (1970)].

[9] T. AMANO, M. WAKATANI, and M. WATANABE; J. Phys. Soc. Jap. 33 782 (1972).

Captions of Figures and a Table

Fig.1. A schematic drawing of the apparatus.

Fig.2. Typical waveforms of plasma current I_p and main toroidal magnetic field.

Fig.3. Typical waveforms of output signal from neutral particle analyzer; (a) without plasma current and (b) with plasma current. The particle energy is 600 eV.

Fig.4. A typical Doppler profile of D_α line.

Fig.5. A typical time evolution of plasma parameters measured by various techniques. Here, operation is done under positive bias field. The maximum plasma current and toroidal field are 105 kA and 9 kG, respectively. Circles, T_i from Doppler broadening of D_α; black circles, T_i from Doppler broadening of O-IV 3063 Å line; squares, T_i of lower temperature component obtained by neutral particle energy analyzer; black squares, T_i of higher temperature component obtained by neutral particle energy analyzer; triangles, T_e from laser scattering; black triangles, T_e from SX foil absorption techniques; crosses, n_e from laser scattering.

Fig.6. A schematic drawing of the system of eight magnetic probes around the discharge tube. Signals from magnetic probes are converted into five Fourier components using the relation,

$$B_p(\theta) = d_0/2 + a_1\cos\theta + b_1\sin\theta + a_2\cos2\theta + b_2\sin2\theta.$$

Fig.7. A typical example of output signals from the Fourier analyzer.

Fig.8. Typical examples of time evolution of q, β, amplitude of m = 2 mode ($\sqrt{(a_2^2 + b_2^2)}/d_0$) and sine component of m = 1 mode (b_1/d_0).

(A) an operation of a low q and low β

(B) an operation of a low q and high β

(C) an operation of a high q and low β.

Fig.9. The time evolution of pressure distribution with and without vertical field. Here, max. B_t is 9 kG and max. I_p is 85 kA. Circles, with vertical field; triangles, without vertical field.

Fig.10. The time evolution of the amplitude of m = 2 mode under the operating condition of Fig.9; (a) without vertical field and (b) with vertical field.

Fig.11. The current distribution across the plasma, the operating condition is the same as that of Fig.9 but without vertical field.

Table I. Major dimensions and parameters of the STP system.

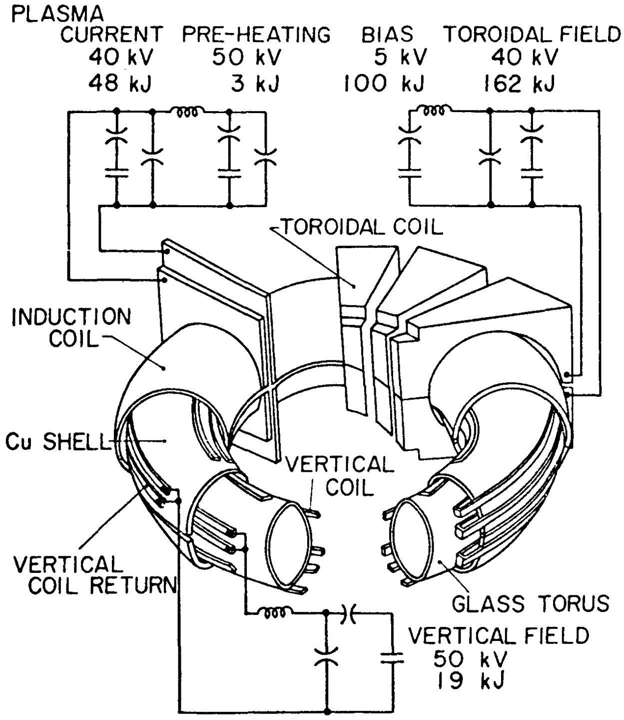

Fig.1. A schematic drawing of the apparatus.

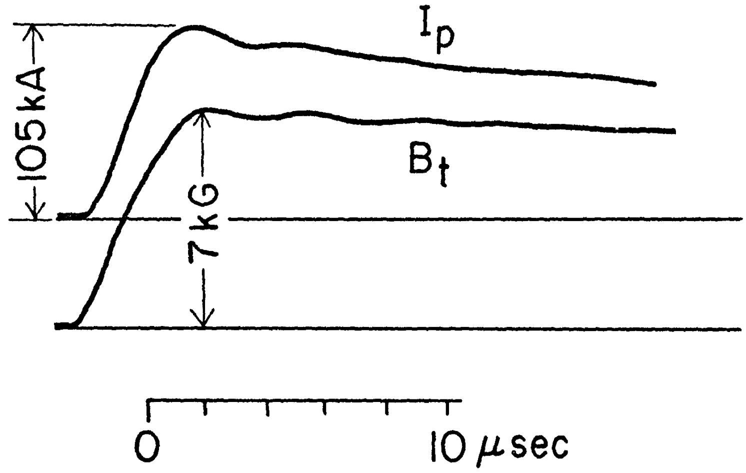

Fig.2. Typical waveforms of plasma current I_p and main toroidal magnetic field.

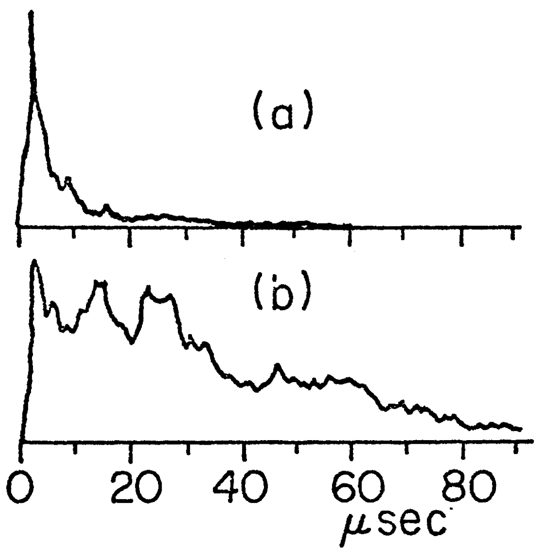

Fig.3. Typical waveforms of output signal from neutral particle analyzer; (a) without plasma current and (b) with plasma current. The particle energy is 600 eV.

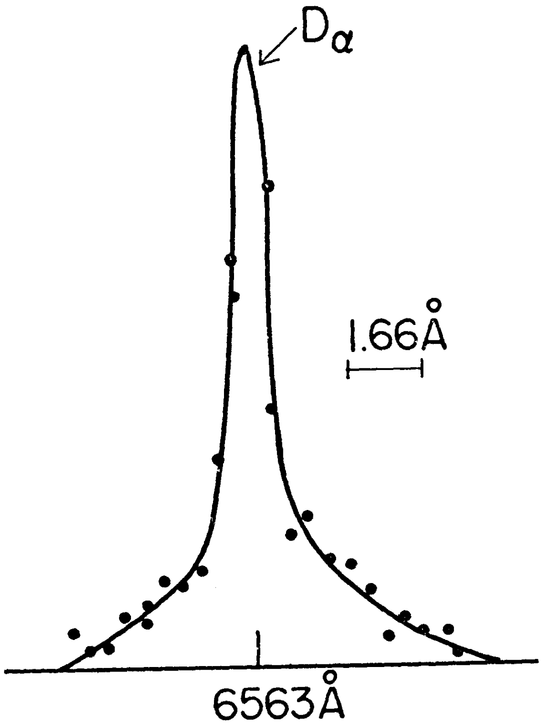

Fig.4. A typical Doppler profile of D_α line.

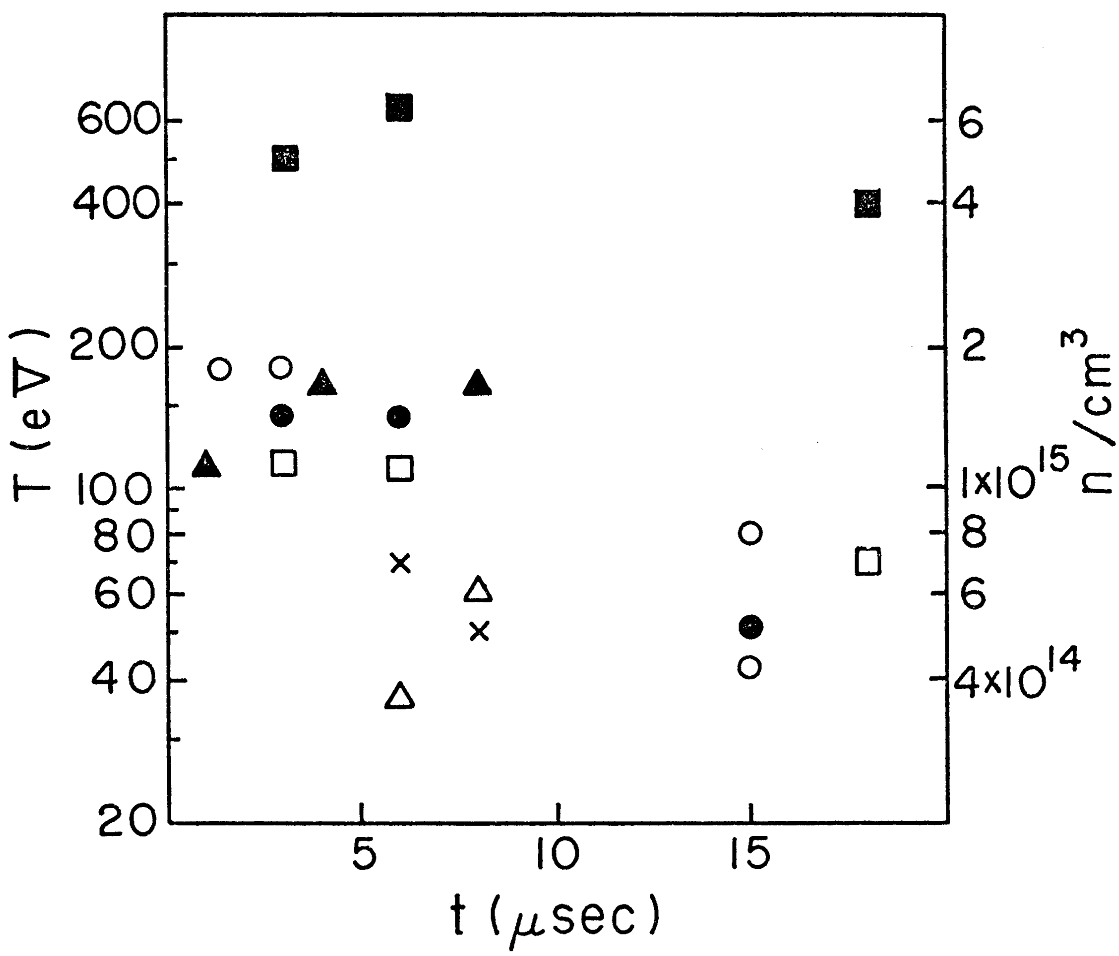

Fig.5. A typical time evolution of plasma parameters measured by various techniques. Here, operation is done under positive bias field. The maximum plasma current and toroidal field are 105 kA and 7 kG, respectively. Circles, T_i from Doppler broadening of D_α; black circles, T_i from Doppler broadening of O-IV 3063 Å line; squares, T_i of lower temperature component obtained by neutral particle energy analyzer; black squares, T_i of higher temperature component obtained by neutral particle energy analyzer; triangles, T_e from laser scattering; black triangles, T_e from SX foil absorption techniques; crosses, n_e from laser scattering.

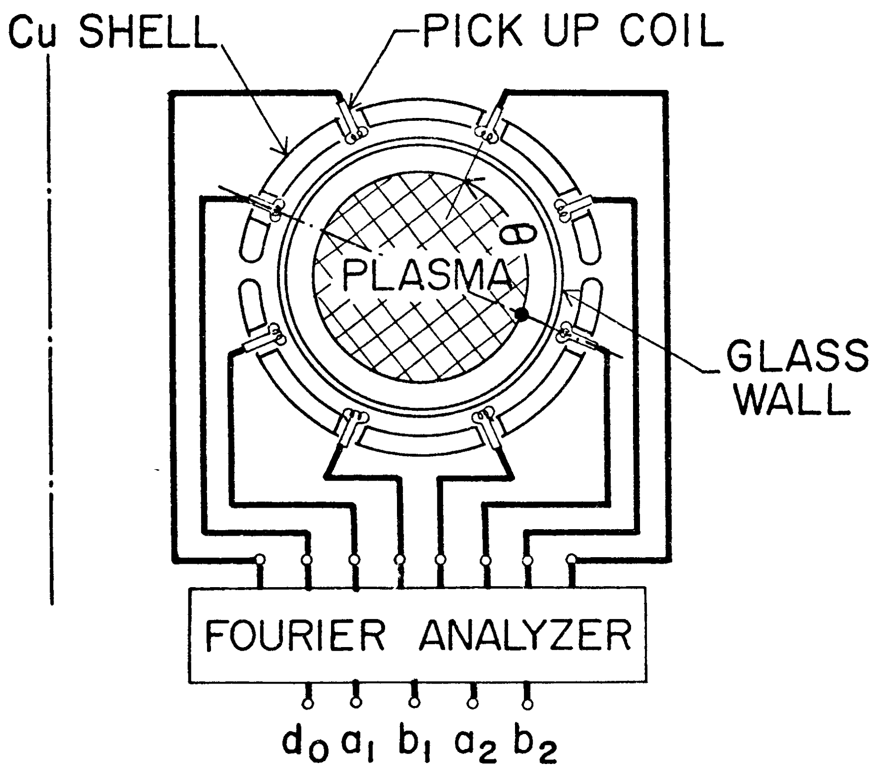

Fig.6. A schematic drawing of the system of eight magnetic probes around the discharge tube. Signals from magnetic probes are converted into five Fourier components using the relation,

$B_p(\theta) = d_0/2 + a_1\cos\theta + b_1\sin\theta + a_2\cos2\theta + b_2\sin2\theta.$

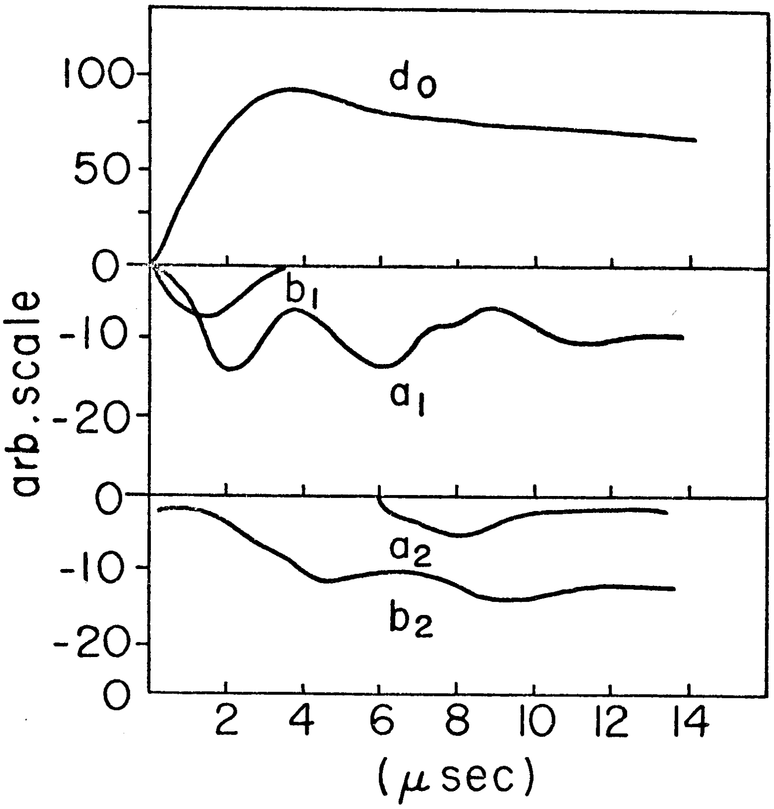

Fig.7. A typical example of output signals from the Fourier analyzer.

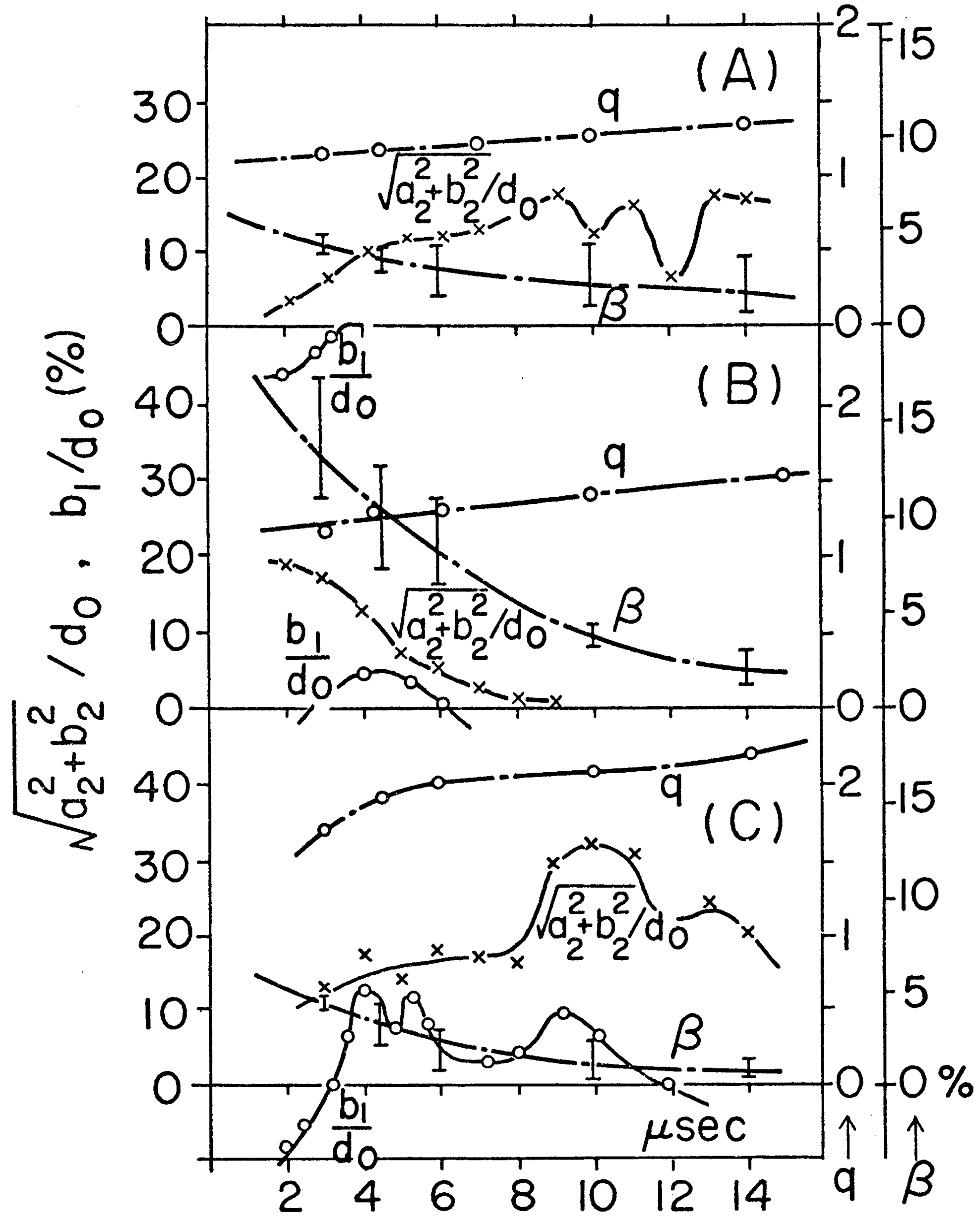

Fig.8. Typical examples of time evolution of q, β, amplitude of m = 2 mode ($\sqrt{a_2^2 + b_2^2}/d_0$) and sine component of m = 1 mode (b_1/d_0).

(A) an operation of a low q and low β

(B) an operation of a low q and high β

(C) an operation of a high q and low β.

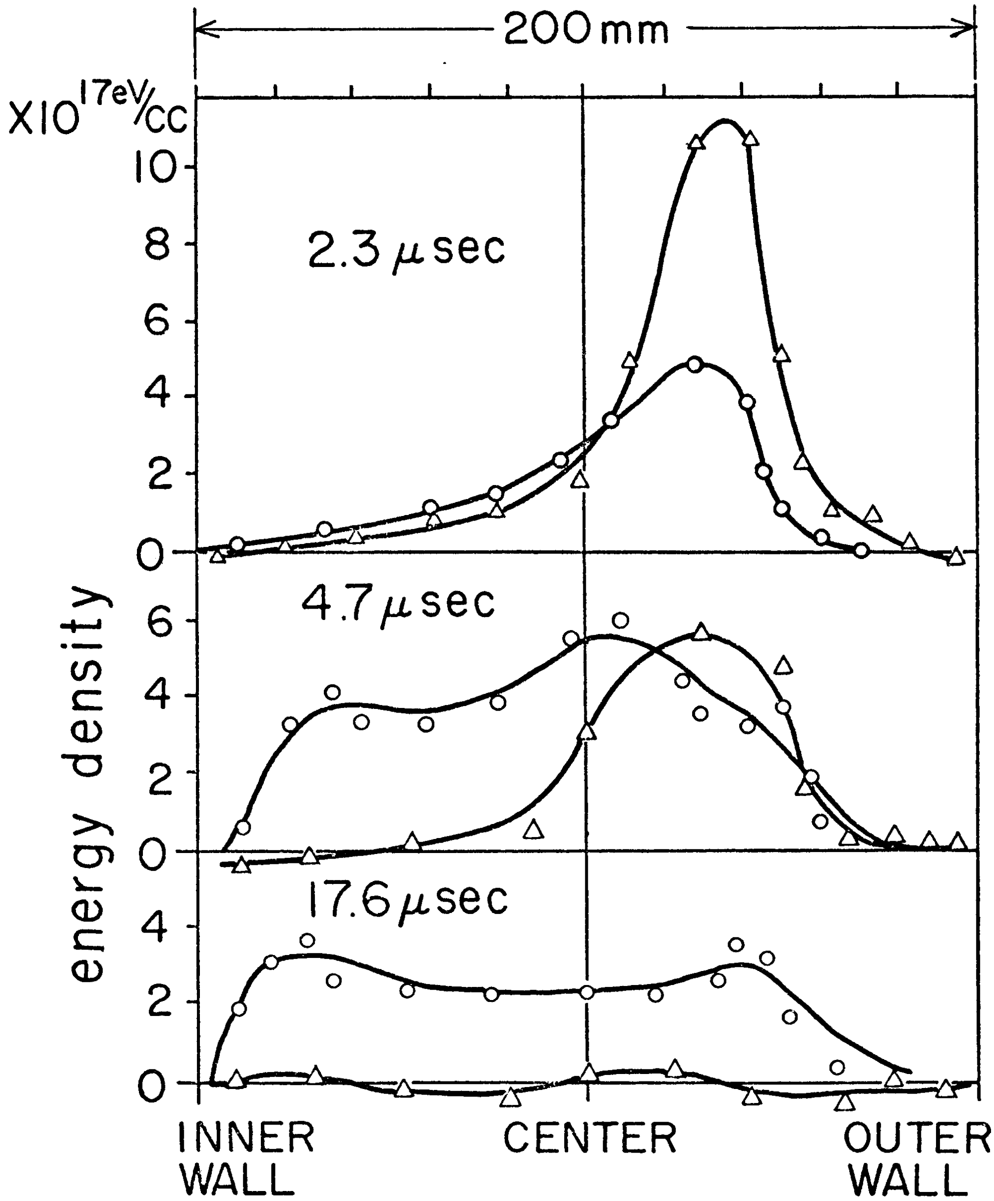

Fig.9. The time evolution of pressure distribution with and without vertical field. Here, max. B_t is 9 kG and max. I_p is 85 kA. Circles, with vertical field; triangles, without vertical field.

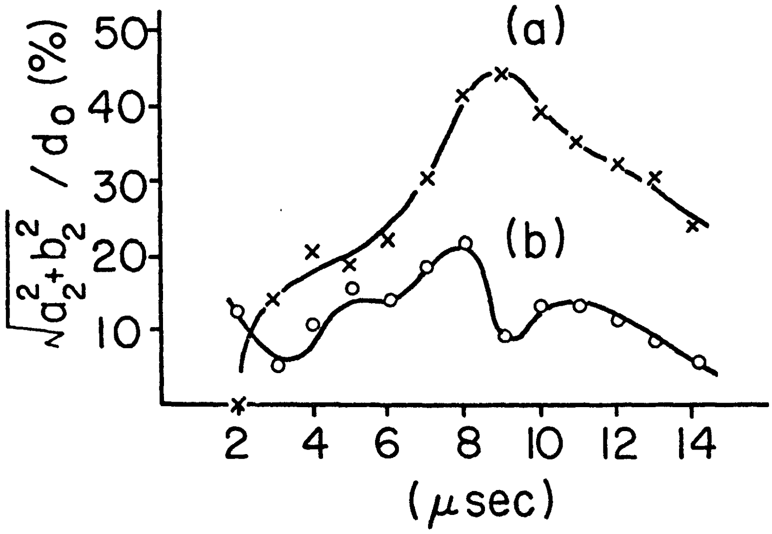

Fig.10. The time evolution of the amplitude of m = 2 mode under the operating condition of Fig.9; (a) without vertical field and (b) with vertical field.

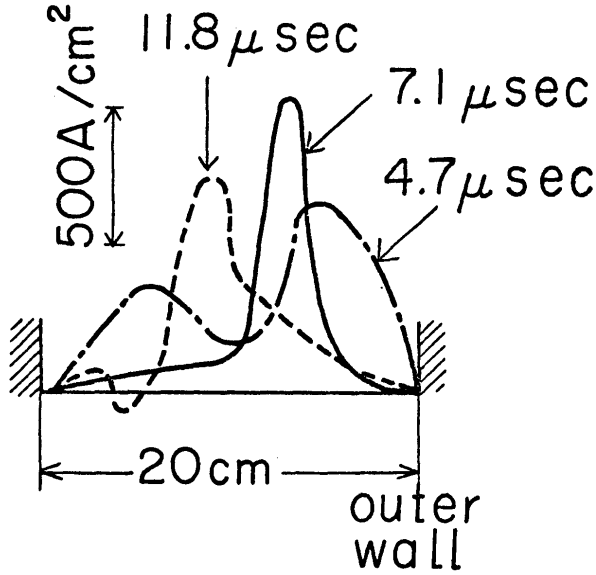

Fig.11. The current distribution across the plasma, the operating condition is the same as that of Fig.9 but without vertical field.

Major radius R (glass torus)	25	cm
Minor radius of glass torus	9.7	cm
Aspect ratio of the torus	2.55	
Max toroidal field B_t	13	kG
Rise time of B_t	3.5	μsec
Decay time of B_t	350	μsec
Max primary current I_z	400	kA
Rise time of I_z	3.5	μsec
Decay time of I_z	170	μsec
Max one-turn voltage around the torus	26	kV
Max bias field	1.3	kG
Max preheating plasma current I_{ph}	30	kA
Decay time of I_{ph}	12	μsec
Max vertical field B_v	480	G
Rise time of B_v	4	μsec

Table I. Major dimensions and parameters of the STP system.

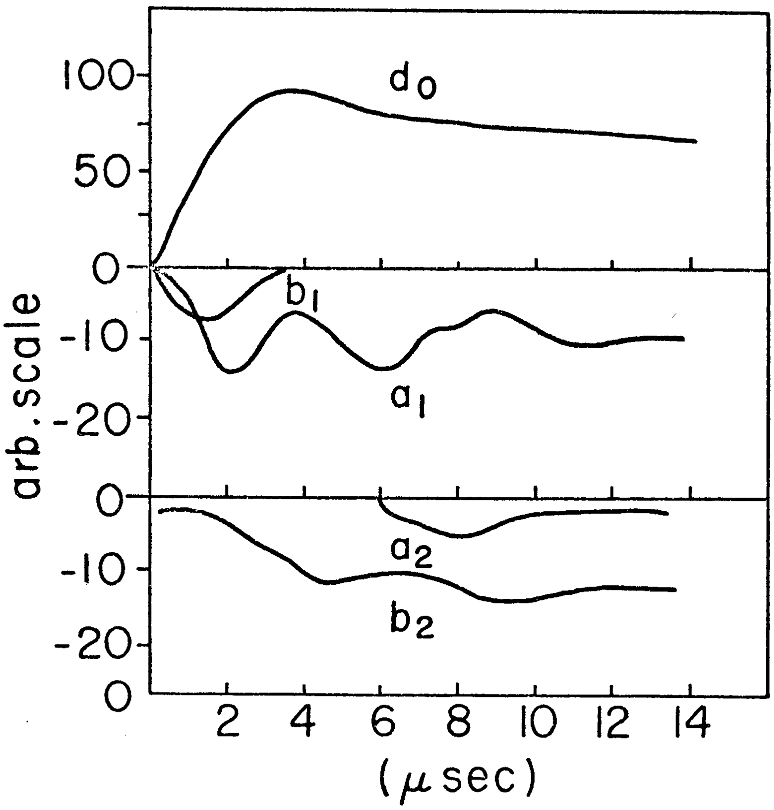

Fig.7. A typical example of output signals from the Fourier analyzer.

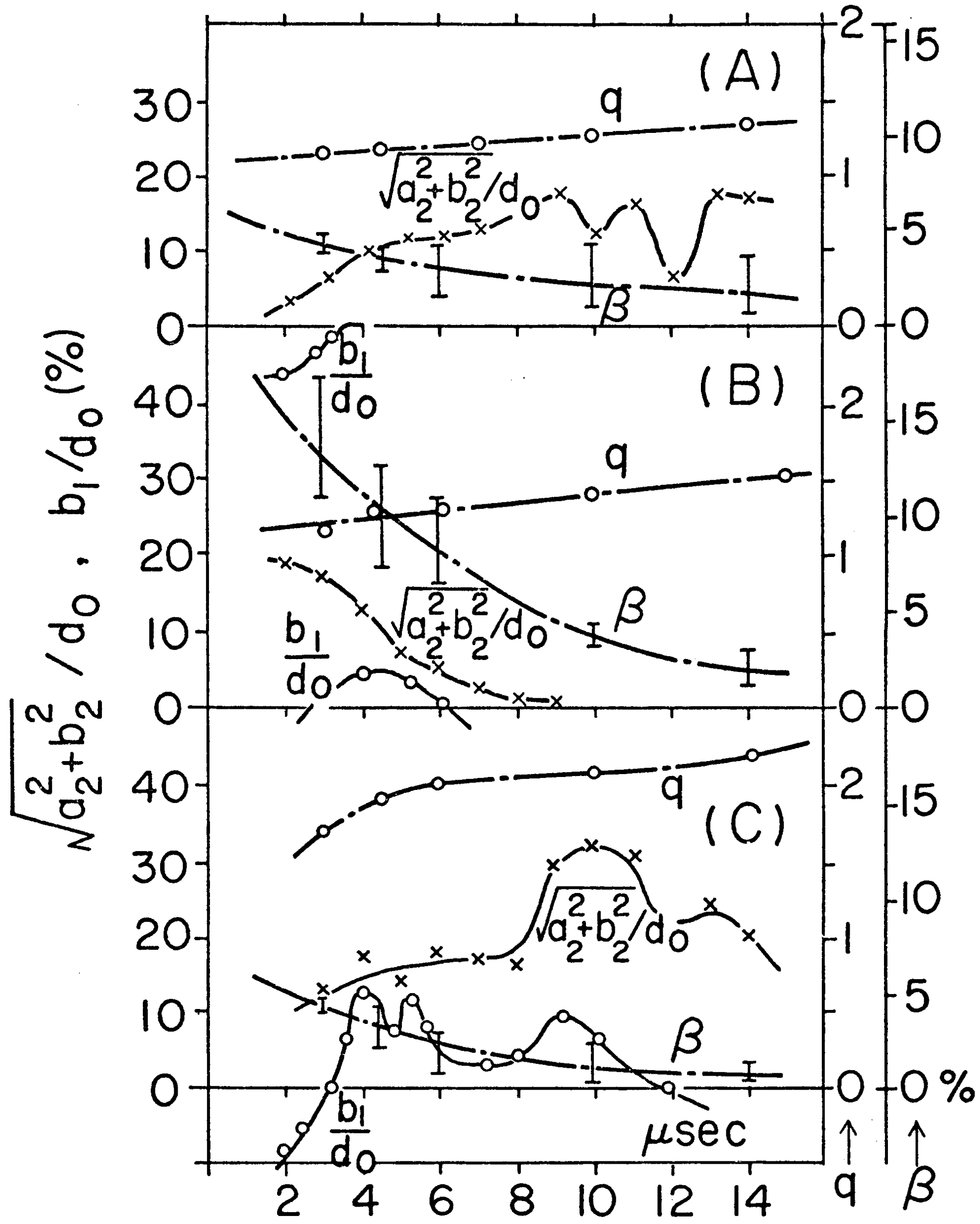

Fig.8. Typical examples of time evolution of q, β, amplitude of m = 2 mode ($\sqrt{a_2^2 + b_2^2}/d_0$) and sine component of m = 1 mode (b_1/d_0).

(A) an operation of a low q and low β

(B) an operation of a low q and high β

(C) an operation of a high q and low β.